The morphology of amyloid fibrils and their impact on tissue damage in hereditary transthyretin amyloidosis: an ultrastructural study

Haruki Koike[a], Ryoji Nishi[a], Shohei Ikeda[a], Yuichi Kawagashira[a], Masahiro Iijima[a], Takeo Sakurai[b], Takayoshi Shimohata[b], Masahisa Katsuno[a], Gen Sobue[a,c]

[a]Department of Neurology, Nagoya University Graduate School of Medicine, Nagoya, Japan

[b]Department of Neurology and Geriatrics, Gifu University Graduate School of Medicine, Gifu, Japan

[c]Research Division of Dementia and Neurodegenerative Disease, Nagoya University Graduate School of Medicine, Nagoya, Japan.

Key words: CIDP; electron microscopy; familial amyloid polyneuropathy; pathogenesis; pathology; Schwann cell; toxicity; ultrastructure

Address correspondence to Haruki Koike, MD, PhD or Gen Sobue, MD, PhD

Department of Neurology, Nagoya University Graduate School of Medicine, Nagoya 466-8550 Japan

Phone: +81-52-744-2391 or +81-52-744-2794

Fax: +81-52-744-2393 or +81-52-744-2967

E-mail: koike-haruki@med.nagoya-u.ac.jp or sobueg@med.nagoya-u.ac.jp

Abstract

Introduction: We evaluated the morphology of amyloid fibrils in the peripheral nervous system using biopsy or autopsy specimens from hereditary transthyretin amyloidosis patients. The impact of amyloid fibril formation on neighboring tissues was also investigated.

Methods: Sural nerve biopsy specimens from 34 patients were examined using electron microscopy. Twenty-eight patients had Val30Met mutations, and the remaining 6 patients had non-Val30Met mutations (i.e., Glu54Lys, Pro24Ser, Thr49Ala, Val71Ala, Val94Gly, and Ala97Gly). The patients with the Val30Met mutation included a case from Brazil (supposedly of Portuguese origin), 6 early-onset cases from endemic foci in Japan, and 21 late-onset cases from non-endemic areas in Japan.

Results: Long amyloid fibers were abundant in the early-onset Val30Met cases from the Japanese endemic foci and Brazil, whereas the amyloid fibrils were generally short in the late-onset Val30Met and non-Val30Met cases. The amyloid fibrils seemed to mature from dotty structures among amorphous electron-dense extracellular materials and pull surrounding tissues during the maturation process. The distortion of Schwann cells close to amyloid fibril masses was conspicuous, particularly in cases with long amyloid fibrils. Atrophy was conspicuous in non-myelinating Schwann cells and bands of Büngner (i.e., Schwann cell subunits that previously contained myelinated axons), particularly those completely surrounded by amyloid fibrils. In contrast, the myelinated fibers tended to be only partially surrounded by amyloid fibrils and morphologically preserved due to their large size. Only a few demyelinated axons were found.

Conclusion: Pre-fibrillar amyloid precursors appear to play a pivotal role during the initial phase of amyloid fibril formation. The mechanical distortion and subsequent atrophy of Schwann cells resulting from the elongation of amyloid fibrils may be

related to small-fiber predominant loss, which is a classical characteristic of amyloid neuropathy. Although rather rare, the destruction of myelin (i.e., demyelination) resulting from amyloid deposition may relate to nerve conduction abnormalities mimicking chronic inflammatory demyelinating polyneuropathy.

Introduction

Hereditary (variant) transthyretin (ATTRv) amyloidosis, also known as familial amyloid polyneuropathy (FAP), is a disease in which systemic deposition of amyloidogenic mutant TTR protein causes multi-organ failure. Although Val30Met is the most common mutation in ATTRv amyloidosis, over 130 other mutations have been reported thus far [1]. The TTR protein is mainly produced in the liver but is also produced in the choroid plexus and retinal pigment epithelium and is stable in the homotetramer form [2]. The dissociation of TTR tetramers is a crucial step in the formation of amyloid fibrils [2]. The process of amyloid formation in ATTRv amyloidosis has been well investigated *in vitro*, and a therapeutic strategy to stabilize TTR tetramers in the plasma is now available in clinical practice [3].

However, the *in vivo* mechanisms of tissue damage resulting from mutant TTR have not been fully elucidated. Although some studies highlight the toxicity of pre-fibrillar TTR (i.e., the precursor of amyloid fibrils) [4-7], the amyloid deposits are more widely believed to exert harmful effects on neighboring tissues [7-11]. Previous studies have demonstrated differences in the morphology of amyloid fibrils in ATTRv amyloidosis patients with the Val30Met mutation depending on the age at onset [7,12,13]. In Japanese ATTRv amyloidosis patients with the Val30Met mutation, long and thick amyloid fibrils are common in early-onset cases from endemic foci, whereas the fibrils are usually short and thin in late-onset cases from non-endemic areas [7,13]. As the neuropathic features and modality of the nerve fiber loss in these two forms of ATTRv amyloidosis are distinct [6,14], the difference in the morphology of the amyloid fibrils may be strongly related to the mechanisms of its neuropathy.

In the present study, we evaluated the electron microscopic morphology of amyloid fibrils in the peripheral nervous system using biopsy or autopsy specimens from various

types of ATTRv amyloidosis patients. We also evaluated the impact of the amyloid fibrils on neighboring tissues in these patients.

Patients and methods

Patients

Biopsy or autopsy specimens from 34 patients with ATTRv amyloidosis who were referred to Nagoya University Graduate School of Medicine and exhibited endoneurial amyloid deposits on electron microscopic examinations were investigated. The patients included 28 patients with the Val30Met mutation and 6 patients with non-Val30Met mutations (i.e., Glu54Lys, Pro24Ser, Thr49Ala, Val71Ala, Val94Gly, and Ala97Gly) (Table 1). The patients with the Val30Met mutation included a 42-year-old man from Brazil, 6 early-onset cases from endemic foci in Japan, and 21 late-onset cases from non-endemic areas in Japan. Since the case from Brazil was a first-generation immigrant to Japan without any apparent Japanese blood relatives, his disease was considered to have originated in Portugal [15]. Except for the patients with the Val94Gly and Ala97Gly mutations, who were autopsied, the specimens were obtained at diagnostic sural nerve biopsy. Autopsy findings in Val94Gly and Ala97Gly patients were previously published [16,17]. In these patients, cardiac amyloid deposition was conspicuous as in late-onset Val30Met patients from non-endemic areas of Japan [6]. Amyloid deposition and myelinated fibrer loss in the ventral and dorsal spinal roots were minimal or not apparent. Mild to moderate degrees of amyloid deposition and neuronal loss in the parenchyma of the dorsal root ganglia and thoracic sympathetic ganglia were seen. In the median and sciatic/tibial nerves, amyloid deposition in the endoneurium was mild to moderate, and myelinated fiber loss was severe in both patients. Six early-onset Val30Met cases from endemic foci in Japan and 19 late-onset

Val30Met cases from non-endemic areas in Japan were included in a previous study [7]. Informed consent was obtained, and this study was approved by the Ethics Committees of Nagoya University Graduate School of Medicine and conformed to the Ethical Guidelines for Medical and Health Research Involving Human Subjects endorsed by the Japanese government.

Pathological assessment

Biopsy of the sural nerve was performed as previously described [6,7,18]. The specimens were divided into two portions. The first portion was fixed in 2.5% glutaraldehyde in 0.125 M cacodylate buffer (pH 7.4) and embedded in epoxy resin for ultrastructural assessments. The epoxy resin-embedded specimens were cut into ultra-thin transverse sections and stained with uranyl acetate and lead citrate for electron microscopic observation. In this study, the morphology of the amyloid fibrils in the endoneurium was assessed, and at least 6 fascicles were assessed in each case. In this study, amyloid deposits were defined as aggregations of non-branching fibrils in the extracellular space [7]. In addition to the amyloid fibrils, the morphology of the Schwann cells was examined, focusing on their relationship to neighboring amyloid deposits. Schwann cells associated with unmyelinated fibers were designated non-myelinating Schwann cells in this study. The bands of Büngner, which were defined as Schwann cell subunits that previously contained myelinated axons, were distinguished by the following morphologic criteria [19]: (1) the subunits had a larger diameter (3 to 8 μm) than the subunits that formerly contained unmyelinated axons; (2) their profiles were larger than those of the subunits of the non-myelinating Schwann cells; (3) they contained remnants of myelin and lamellated inclusions, suggesting the presence of degeneration; and (4) their shape was more irregular, and their basement

membrane was folded. The second portion of the specimen was fixed in a 10% formalin solution and embedded in paraffin. The sections were cut by routine methods and stained with hematoxylin and eosin and Congo red.

Among the patients with the Val94Gly and Ala97Gly mutations who were autopsied, the median and sciatic/tibial nerves were obtained and processed as previously described [20].

Results

Morphology of amyloid fibrils

In general, amyloid deposits were observed both with and without a relationship to the endoneurial microvessels, although they tended to be present around them. As described in previous studies [7,13], the morphology of the amyloid fibrils of the Japanese early-onset Val30Met cases from endemic foci were distinctly different from the late-onset Val30Met cases from non-endemic areas. The amyloid deposits were burred in the low-power view and mainly consisted of long and thick fibers in the high-power views in all early-onset cases from the endemic foci in Japan (Fig. 1A). Although it is difficult to quantify the exact length of amyloid fibrils taking the thickness of ultrathin sections used for electron microscopic observation (approximately 70 nm), some of the amyloid fibers obviously exceeded 1 μm in length. In contrast, the amyloid deposits tended to show cotton- or cloud-like appearances in the low-power views in the late-onset cases from the non-endemic areas, and in these cases, the amyloid fibrils were usually short and thin and arranged in mesh-like structures on the high-power view (Fig. 1B). The length of amyloid fibrils usually do not exceeded 200 nm in these cases. However, in addition to having short and thin amyloid fibrils, 1 of the 2 women (age at onset, 56 years) and 2 of the 19 men (age at onset, 56 and 60 years) among these

late-onset cases had relatively long and thick fibers, similar to those in the early-onset cases.

Regarding the Brazilian Val30Met patient who supposedly was of Portuguese origin, long and thick fibers were observed, similar to those observed in the early-onset Val30Met cases from the endemic foci in Japan (Fig. 1C). In contrast, the morphology of the amyloid fibrils in the patients with non-Val30Met mutations (i.e., Glu54Lys, Pro24Ser, Thr49Ala, Val71Ala, Val94Gly, and Ala97Gly) was similar to that in the late-onset Val30Met cases from the non-endemic areas in Japan. In these cases, the amyloid fibrils were generally short, although the thickness varied depending on the individual case (Fig. 1D to 1I). The length of the amyloid fibrils seems to be unrelated to the age at onset or time of examination in these non-Val30Met cases; even those examined before 50 years of age showed short fibrils. In autopsied Val94Gly and Ala97Gly cases, median and sciatic/tibial nerves were examined from the proximal to distal portions. Amyloid fibrils were generally short and thin at any portions of these nerves. Amorphous materials were also present at any portions.

Evolution of amyloid fibrils

During the amyloid fibril formation process, amorphous electron-dense extracellular materials seem to play a pivotal role during the initial phase of amyloid fibril formation. Amorphous electron-dense extracellular materials are present in all parts of the endoneurium but are particularly frequent in the subperineurial space and in the vicinity of endoneurial microvessels (Fig. 2A). These amorphous materials were extensively present in some areas, but small patchy deposits were also found. Occasionally, amorphous materials surrounded the myelinating and non-myelinating Schwann cells. Consequently, some portions of their basement membranes became indistinct and

appeared to be continuous with the amorphous materials.

Among these extracellular amorphous materials, dotty or fine fibrillar structures were often observed, particularly in the early-onset Val30Met cases from the endemic foci in Japan and the Brazilian Val30Met case who had long amyloid fibrils (Fig. 2B). The dotty structures seemed to be premature amyloids because slightly elongated fibrillar structures with a thickness similar to the diameter of these dots were also frequently found (Fig. 2C). These short amyloid fibrils had a thickness similar to that of long, mature amyloid fibers. The mature long fibers tended to be located in the central part of the large aggregations of amyloid fibrils, while the amorphous materials, dotty structures, and short fibrils were present at the periphery of the aggregates of amyloid fibrils. However, aggregations of amyloid fibrils unaccompanied by amorphous materials were also found. In the late-onset Val30Met cases and non-Val30Met cases exhibiting short amyloid fibrils, amorphous materials were also frequently found. However, the previously described putative chronological sequence of the evolution of the amyloid fibrils was difficult to imagine in these cases because the amyloid fibrils were generally too small, even in their mature form. Because the amyloid fibrils seemed to pull on the surrounding tissues during their maturation process, the Schwann cells, particularly non-myelinating Schwann cells located around the amyloid fibrils mass, tended to be distorted towards the centers of the amyloid deposits, particularly in cases with long amyloid fibers (Fig. 2D).

Impact of amyloid fibril formation on neighboring tissues

The amyloid fibrils located in the vicinity of Schwann cells seemed to pull on the basement membrane of the Schwann cells as they matured into long fibers (Fig. 3A). The basement membranes were occasionally confluent with the amyloid fibrils. Even

the cytoplasmic membranes were indistinct in these locations (Fig. 3B). The cytoplasm of Schwann cells adjacent to the basement membrane apposed to the amyloid fibrils became atrophic. This atrophy seemed to be more conspicuous in the early-onset Val30Met cases from the endemic foci in Japan and the Brazilian Val30Met case, which had long fibers. Schwann cells completely surrounded by aggregations of amyloid fibrils were also found. Atrophy was conspicuous in these Schwann cells, and their contours comprising basement and cytoplasmic membranes became obscure. Some Schwann cell contours completely disappeared, and only cytoplasmic organelles remained among the aggregation of amyloid fibrils (Fig. 3C). These findings tended to be observed in non-myelinating Schwann cells and bands of Büngner (i.e., Schwann cell subunits that previously contained myelinated axons). As myelinated fibers, particularly large myelinated fibers, are larger than non-myelinating Schwann cells and bands of Büngner, amyloid fibrils rarely siege completely these fibers (Fig. 4A and 4B). Hence, the apposition of myelinated fibers to amyloid fibril aggregates was usually partial. Occasionally, the basement and cytoplasmic membranes of myelinating Schwann cells apposed to amyloid fibrils were obscure, similar to those of the non-myelinating Schwann cells, and their contours became irregular as if they were pulled by the amyloid fibrils (Fig. 4C and 4D). In contrast, such distortion of Schwann cells was less conspicuous in the late-onset Val30Met cases and non-Val30Met cases exhibiting short amyloid fibrils.

Disproportionately large unmyelinated axons > 3 μm in diameter were found in two early-onset Val30Met and three late-onset Val30Met cases from Japan. These axons might be considered to have originally been myelinated and to have undergone demyelination [19]. Naked axons surrounded by amyloid fibrils were found in one of the late-onset Val30Met cases (Fig. 5).

Discussion

In this study, we evaluated the morphology and effect of amyloid fibrils on neighboring tissues in the peripheral nervous system using biopsy or autopsy specimens from patients with ATTRv amyloidosis. Previous studies have described the presence of TTR-positive amorphous extracellular materials in the endoneurium in ATTRv amyloidosis patients and have suggested the significance of these materials as an early lesion before the formation of fibrillar structures [4,6]. Animal studies have also supported this hypothesis [5,21]. Our observations suggest that these extracellular amorphous materials might be the cradles of amyloid fibrils.

The amyloid fibrils were morphologically characterized as being typically long in the early-onset Val30Met cases from the Japanese endemic foci and Brazil, whereas they were short in the other cases. Importantly, the electron microscopic findings of amyloid fibrils and the mode of neighboring tissue damage were similar between the early-onset Val30Met cases from the Japanese endemic foci and the case from Brazil that was considered of Portuguese origin. An early study demonstrated electron microscopic findings of sural nerve biopsy specimens from Portuguese ATTRv amyloidosis patients [8]. Although we did not find any amyloid fibril penetration of Schwann cell membranes and invasion into the Schwann cell cytoplasm, as reported in that study, our findings are consistent with those of the previous study. A haplotype analysis of the *TTR* gene has suggested a common foundation between early-onset patients from Japanese endemic foci and Portuguese patients but not late-onset patients from Japanese non-endemic areas [22].

Previous studies involving patients with Val30Met mutations in Sweden and Japan have revealed that the presence of long amyloid fibers was a characteristic feature in

early-onset cases, while short fibrils were characteristic of late-onset cases [7,12,13]. Short fibrils have also been reported in cardiac amyloid deposits due to senile systemic amyloidosis (i.e., ATTRwt amyloidosis) [23]. In our study, the non-Val30Met patients also had short amyloid fibrils regardless of the age at onset and pathological examination. Regarding the non-Val30Met mutation, the numbers of both the patients and mutations examined in this study were small. Hence, some other non-Val30Met mutation may be characterized by long amyloid fibers. Further large-scale studies are needed to investigate cases with non-Val30Met mutations.

However, at least in our non-Val30Met cases, the changes in the environmental factors in the extracellular space that trigger amyloid formation may be similar to those in ATTRwt amyloidosis and late-onset Val30Met ATTRv amyloidosis. Previous studies have demonstrated the deposition of truncated TTR as amyloid in patients with ATTRwt amyloidosis [23,24]. Interestingly, such truncated TTR also constitutes amyloid deposits in Swedish and Japanese late-onset Val30Met ATTRv amyloidosis patients [12,25]. In contrast, full-length TTR deposits as amyloid have been found in early-onset Val30Met ATTRv amyloidosis patients from these countries [12,25]. Another notable difference in the characteristics of amyloid deposits is the ratio of mutant TTR to wild-type TTR in the amyloid deposits. In hearts from Japanese Val30Met ATTRv amyloidosis patients, most TTR is mutated in early-onset cases from endemic foci, whereas more than half of the TTR is wild-type in late-onset cases from non-endemic areas [13]. These findings may indicate that age-dependent changes in the microenvironment of interstitial tissues similar to ATTRwt amyloidosis determine the characteristics of amyloid deposits in Swedish and Japanese late-onset Val30Met ATTRv amyloidosis. To support this view, amyloid fibrils in ATTRwt amyloidosis patients are morphologically similar to those in Swedish and Japanese late-onset

Val30Met ATTRv amyloidosis patients [23]. Hence, the truncation of TTR and the ratio of mutant TTR to wild-type TTR may determine the size of the amyloid fibrils.

The mechanism by which amyloid fibrils exert harmful effects on surrounding tissues has not been fully elucidated. Electron microscopic observations have shown indistinct Schwann cell basement membranes contiguous to amyloid fibrils, suggesting that amyloid fibrils directly damage Schwann cells in ATTRv amyloidosis [7,8,10,11]. Distorted Schwann cell processes located around amyloid deposits have also been reported [9]. As similar findings have also been reported in light chain amyloidosis (i.e., AL amyloidosis) [26-28], the direct damage on Schwann cells caused by amyloid fibrils may be a common mechanism underlying nerve fiber loss in amyloid neuropathy. The destruction of myelin composed of layers of Schwann cells has also been shown by teased-fiber preparations [10]. This myelin destruction may relate to nerve conduction abnormalities that mimic chronic inflammatory demyelinating polyneuropathy (CIDP). Although the main electrophysiological characteristics of ATTRv amyloidosis are those suggestive of axonal degeneration, slowing of nerve conduction velocities and prolongation of distal motor latencies may coexist [29,30]. We also found demyelinated axons surrounded by amyloid fibrils although they were rare. Such myelin destruction resulting from amyloid deposition may relate to electrophysiological abnormalities mimicking CIDP.

In our study, amyloid fibrils seemed to be formed among electron-dense amorphous materials located in extracellular spaces. The various components of the amorphous material located around the amyloid may become assembled and organized into mature amyloid fibrils, as has been previously suggested by other scholars [31]. Hence, amyloid deposits may pull surrounding tissues during the process of fibril formation, particularly elongation. Distorted Schwann cell processes adjacent to amyloid fibril

masses were more frequently observed in the early-onset Val30Met patients who had long amyloid fibrils than in those with short amyloid fibrils. We hypothesize that the traction of surrounding tissues by amyloid fibrils becomes more conspicuous as the fibrils become larger. In addition to the direct toxicity of amyloid fibrils [32], this mechanical distortion of surrounding tissues resulting from the process of amyloid fibril formation may participate in the tissue damage, particularly in smaller diameter nerve fibers.

Acknowledgments

This work was supported by grants from the Ministry of Health, Labor and Welfare (Research on Rare and Intractable Diseases, H29-022) and the Ministry of Education, Culture, Sports, Science and Technology (17K09777) of Japan.

Disclosure statement

The authors have no conflicts of interest to declare.

References

[1] Sekijima Y, Ueda M, Koike H, et al. Diagnosis and management of transthyretin familial amyloid polyneuropathy in Japan: red-flag symptom clusters and treatment algorithm. Orphanet J Rare Dis. 2018;13:6.

[2] Ueda M, Ando Y. Recent advances in transthyretin amyloidosis therapy. Transl Neurodegener. 2014;3:19.

[3] Adams D, Cauquil C, Labeyrie C. Familial amyloid polyneuropathy. Curr Opin Neurol. 2017;30:481-489.

[4] Sousa MM, Cardoso I, Fernandes R, et al. Deposition of transthyretin in early stages of familial amyloidotic polyneuropathy: evidence for toxicity of nonfibrillar aggregates. Am J Pathol. 2001;159:1993-2000.

[5] Sousa MM, Fernandes R, Palha JA, et al. Evidence for early cytotoxic aggregates in transgenic mice for human transthyretin Leu55Pro. Am J Pathol. 2002;161:1935-1948.

[6] Koike H, Misu K, Sugiura M, et al. Pathology of early- vs late-onset TTR Met30 familial amyloid polyneuropathy. Neurology. 2004;63:129-138.

[7] Koike H, Ikeda S, Takahashi M, et al. Schwann cell and endothelial cell damage in transthyretin familial amyloid polyneuropathy. Neurology. 2016;87:2220-2229.

[8] Coimbra A, Andrade C. Familial amyloid polyneuropathy: an electron microscope study of the peripheral nerve in five cases. I. Interstitial changes. Brain. 1971;94:199-206.

[9] Thomas PK, King RH. Peripheral nerve changes in amyloid neuropathy. Brain. 1974;97:395-406.

[10] Said G, Ropert A, Faux N. Length-dependent degeneration of fibers in Portuguese amyloid polyneuropathy: a clinicopathologic study. Neurology. 1984;34:1025-1032.

[11] Sobue G, Nakao N, Murakami K, et al. Type I familial amyloid polyneuropathy. a

pathological study of the peripheral nervous system. Brain. 1990;113:903-919.

[12] Ihse E, Ybo A, Suhr O, et al. Amyloid fibril composition is related to the phenotype of hereditary transthyretin V30M amyloidosis. J Pathol. 2008;216:253-261.

[13] Koike H, Ando Y, Ueda M, et al. Distinct characteristics of amyloid deposits in early- and late-onset transthyretin Val30Met familial amyloid polyneuropathy. J Neurol Sci. 2009;287:178-184.

[14] Koike H, Misu K, Ikeda S, et al. Type I (transthyretin Met30) familial amyloid polyneuropathy in Japan: early- vs late-onset form. Arch Neurol. 2002;59:1771-1776.

[15] Zaros C, Genin E, Hellman U, et al. On the origin of the transthyretin Val30Met familial amyloid polyneuropathy. Ann Hum Genet. 2008;72:478-484.

[16] Mukai E, Ichihara S, Yoshida M, et al. Transthyretin-type amyloidosis (VAL94Gly) with cardiomyopathy: report of an autopsy case. Shinkeinaika. 2007;67:171-177.

[17] Koike H, Yasuda T, Nishi R, et al. Systemic angiopathy and axonopathy in hereditary transthyretin amyloidosis with Ala97Gly (p. Ala117Gly) mutation: a postmortem analysis. Amyloid. in press.

[18] Takahashi M, Koike H, Ikeda S, et al., Distinct pathogenesis in nonsystemic vasculitic neuropathy and microscopic polyangiitis. Neurol Neuroimmunol Neuroinflamm. 2017;4:e407.

[19] Koike H, Iijima M, Mori K, et al., Nonmyelinating Schwann cell involvement with well-preserved unmyelinated axons in Charcot-Marie-Tooth disease type 1A. J Neuropathol Exp Neurol. 2007;66:1027-1036.

[20] Koike H, Kiuchi T, Iijima M, et al. Systemic but asymptomatic transthyretin amyloidosis 8 years after domino liver transplantation. J Neurol Neurosurg Psychiatry. 2011;82:1287-1290.

[21] Ueda M, Ando Y, Hakamata Y, et al. A transgenic rat with the human ATTR V30M: a novel tool for analyses of ATTR metabolisms. Biochem Biophys Res Commun. 2007;352:299-304.

[22] Ohmori H, Ando Y, Makita Y, et al. Common origin of the Val30Met mutation responsible for the amyloidogenic transthyretin type of familial amyloidotic polyneuropathy. J Med Genet. 2004;41:e51.

[23] Bergström J, Gustavsson A, Hellman U, et al. Amyloid deposits in transthyretin-derived amyloidosis: cleaved transthyretin is associated with distinct amyloid morphology. J Pathol. 2005;206:224-232.

[24] Westermark P, Bergström J, Solomon A, et al. Transthyretin-derived senile systemic amyloidosis: clinicopathologic and structural considerations. Amyloid. 2003;10(Suppl 1):48-54.

[25] Oshima T, Kawahara S, Ueda M, et al. Changes in pathological and biochemical findings of systemic tissue sites in familial amyloid polyneuropathy more than 10 years after liver transplantation. J Neurol Neurosurg Psychiatry. 2014;85:740-746.

[26] Vital C, Vallat JM, Deminiere C, et al. Peripheral nerve damage during multiple myeloma and Waldenstrom's macroglobulinemia: an ultrastructural and immunopathologic study. Cancer. 1982;50:1491-1497.

[27] Sommer C, Schröder JM. Amyloid neuropathy: immunocytochemical localization of intra- and extracellular immunoglobulin light chains. Acta Neuropathol. 1989;79:190-199.

[28] Vallat JM, Vital A, Magy L, et al. An update on nerve biopsy. J Neuropathol Exp Neurol. 2009;68:833-844.

[29] Koike H, Hashimoto R, Tomita M, et al. Diagnosis of sporadic transthyretin Val30Met familial amyloid polyneuropathy: a practical analysis. Amyloid.

2011;18:53-62.

[30] Lozeron P, Mariani LL, Dodet P, et al. Transthyretin amyloid polyneuropathies mimicking a demyelinating polyneuropathy. Neurology. in press.

[31] Inoue S, Kuroiwa M, Saraiva MJ, et al. Ultrastructure of familial amyloid polyneuropathy amyloid fibrils: examination with high-resolution electron microscopy. J Struct Biol. 1998;124:1-12.

[32] Ando Y, Nyhlin N, Suhr O, et al. Oxidative stress is found in amyloid deposits in systemic amyloidosis. Biochem Biophys Res Commun. 1997;232:497-502.

Figure legends

Fig. 1. Morphology of amyloid fibrils in the endoneurium of biopsy or autopsy specimens from patients with ATTRv amyloidosis (observed at the same magnification). (A) Early-onset Val30Met case from an endemic focus in Japan, (B) late-onset Val30Met case from a non-endemic area in Japan, (C) Val30Met case from Brazil (supposedly of Portuguese origin), (D) Glu54Lys case, (E) Pro24Ser case, (F) Thr49Ala case, (G) Val71Ala case, (H) Val94Gly case, and (I) Ala97Gly case. Amyloid fibrils tend to be long in the early-onset cases from an endemic focus in Japan (A) and Val30Met case from Brazil (C), while they are generally short in the late-onset Val30Met case from a non-endemic area in Japan (B) and non-Val30Met cases (D to I). Uranyl acetate and lead citrate stain. Scale bars = 0.2 μm.

Fig. 2. Putative chronological sequence of amyloid fibril formation and subsequent impact on surrounding tissues. Cross sections of sural nerve biopsy specimens from the early-onset Val30Met cases from the endemic foci in Japan. (A) Dotty structures (arrow), which seemed to be premature amyloids, were often observed among the amorphous electron-dense extracellular materials. A high-powered view of the box in (A) is shown in (B). (C) Slightly elongated fibrillar structures with a thickness similar to the diameter of the dotty structures were also frequently found. (D) As the amyloid fibrils seemed to pull the surrounding tissues during their maturation process, non-myelinating Schwann cells located around the mass of amyloid fibrils tended to be distorted towards the center of the amyloid deposits. Uranyl acetate and lead citrate stain. Scale bars = 0.2 μm (A and C), 0.1 μm (B), and 2 μm (D).

Fig. 3. Schwann cell damage resulting from amyloid fibril formation in the early-onset

Val30Met case from an endemic focus in Japan (A) and the Val30Met case from Brazil (B and C). Cross sections of sural nerve biopsy specimens. (A) Amyloid fibrils located in the vicinity of Schwann cells seemed to pull the basement membrane of the Schwann cells in the direction indicated by the arrows as they matured into long fibers. Basement membranes were occasionally confluent with amyloid fibrils. (B) Even cytoplasmic membranes became indistinct, and the contours of Schwann cells consisting of basement and cytoplasmic membranes became obscure. (C) Some Schwann cell contours completely disappeared, and only cytoplasmic organelles remained among the aggregation of amyloid fibrils (arrowheads). Uranyl acetate and lead citrate stain. Scale bars = 0.2 μm (A and B) and 0.5 μm (C).

Fig. 4. Impact of amyloid deposition on myelinated fibers. Cross sections of sural nerve biopsy specimens from the Val30Met case from Brazil (A and B) and the early-onset Val30Met case from an endemic focus in Japan (C and D). (A) As myelinated fibers (arrow), particularly large myelinated fibers, are larger than non-myelinating Schwann cells (arrowheads), amyloid fibrils rarely siege completely these fibers. Hence, the apposition of myelinated fibers to aggregates of amyloid fibrils was usually partial. A high-powered view of the box in (A) is shown in (B). (C) The basement and cytoplasmic membranes of myelinating Schwann cells apposed to amyloid fibrils sometimes became obscure, and their contours occasionally became irregular as if they were pulled by amyloid fibrils. A high-powered view of the box in (C) is shown in (D). Uranyl acetate and lead citrate stain. Scale bars = 2 μm (A and C), 0.5 μm (B), and 0.2 μm (D).

Fig. 5. Demyelinated axon. Cross section of a sural nerve biopsy specimen from the

late-onset Val30Met case from a non-endemic area in Japan. Disproportionately large unmyelinated axon, which was considered to have originally been myelinated, was surrounded by amyloid fibrils. Uranyl acetate and lead citrate stain. Scale bar = 2 μm.

Table 1. Summary of patients

Mutation	Number of patients	Region of origin	Sex	Age at onset (years)	Age at biopsy /autopsy (years)	Morphology of* amyloid fibrils	Atrophy of Schwann cells apposed to amyloid fibrils*
Val30Met	6	Endemic foci in Japan	4 M and 2 F	32.8 ± 4.5**	35.7 ± 4.3**	Long	Conspicuous
Val30Met	21	Non-endemic areas in Japan	19 M and 2 F	64.6 ± 7.5**	68.6 ± 7.6**	Short***	Inconspicuous
Val30Met	1	Brazil	M	39	42	Long	Conspicuous
Glu54Lys	1	Japan	F	42	44	Short	Inconspicuous
Pro24Ser	1	Japan	M	70	75	Short	Inconspicuous
Thr49Ala	1	Japan	F	49	54	Short	Inconspicuous
Val71Ala	1	Brazil	F	31	35	Short	Inconspicuous
Val94Gly	1	Japan	F	58	65	Short	Inconspicuous
Ala97Gly	1	Japan	M	56	74	Short	Inconspicuous

*Sural nerve biopsy specimens were assessed in all patients, except for the patients with the Val94Gly and Ala97Gly mutations. Autopsy specimens of the median and sciatic/tibial nerves were assessed in patients with the Val94Gly and Ala97Gly mutations.

**Values are expressed as the mean ± SD.

***Long fibrils were also found in three patients.

Fig. 1

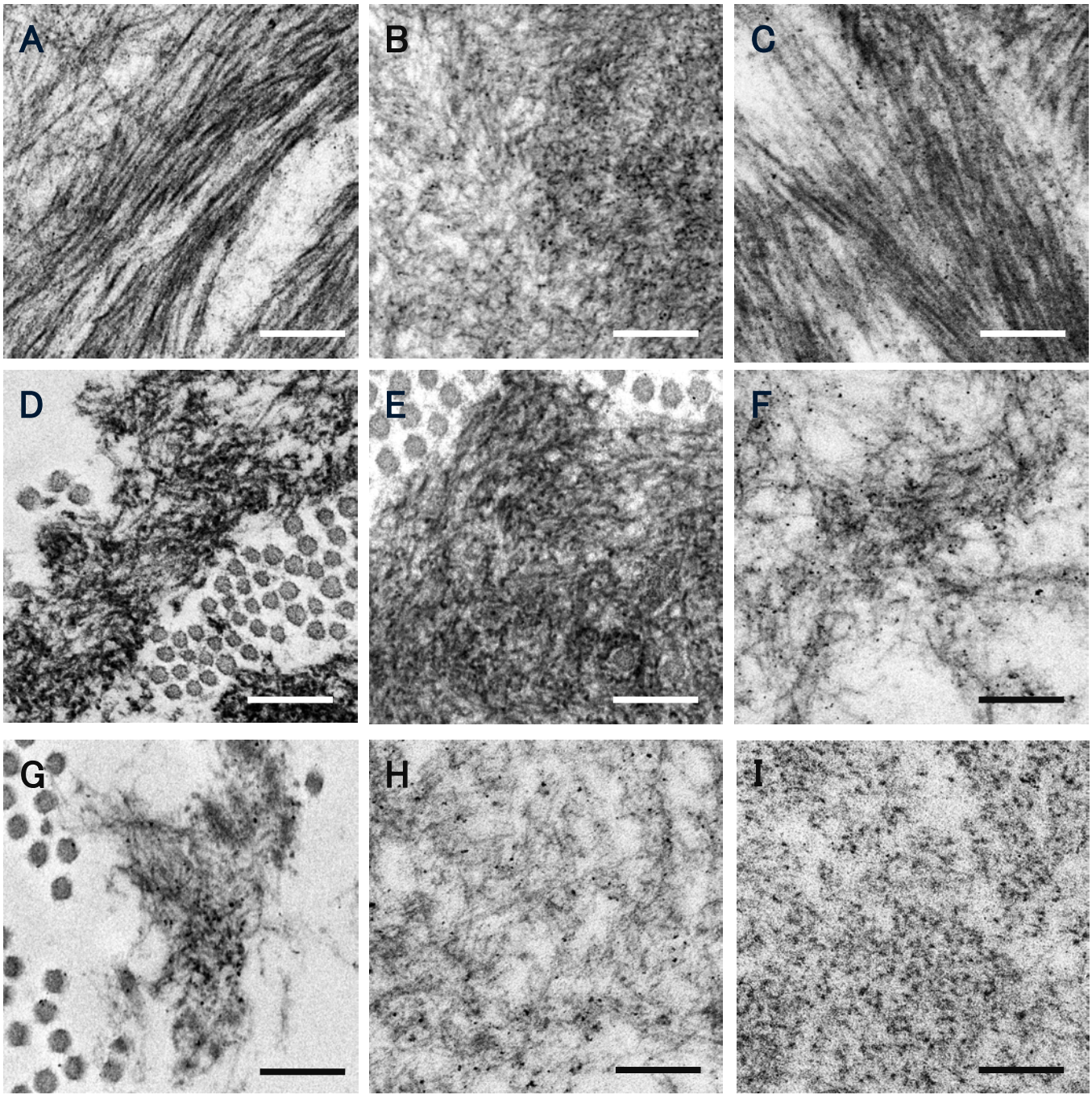

Fig. 2

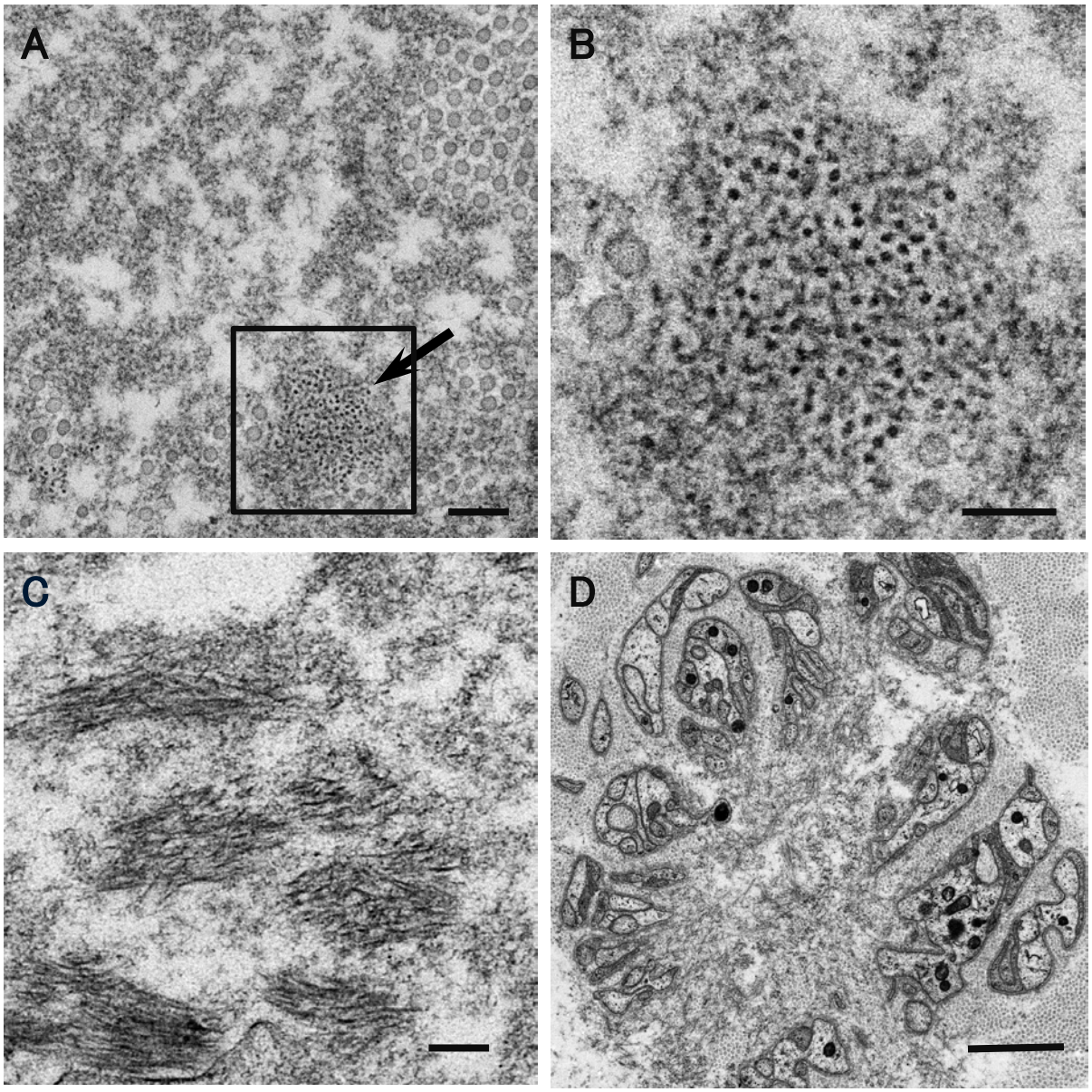

Fig. 3

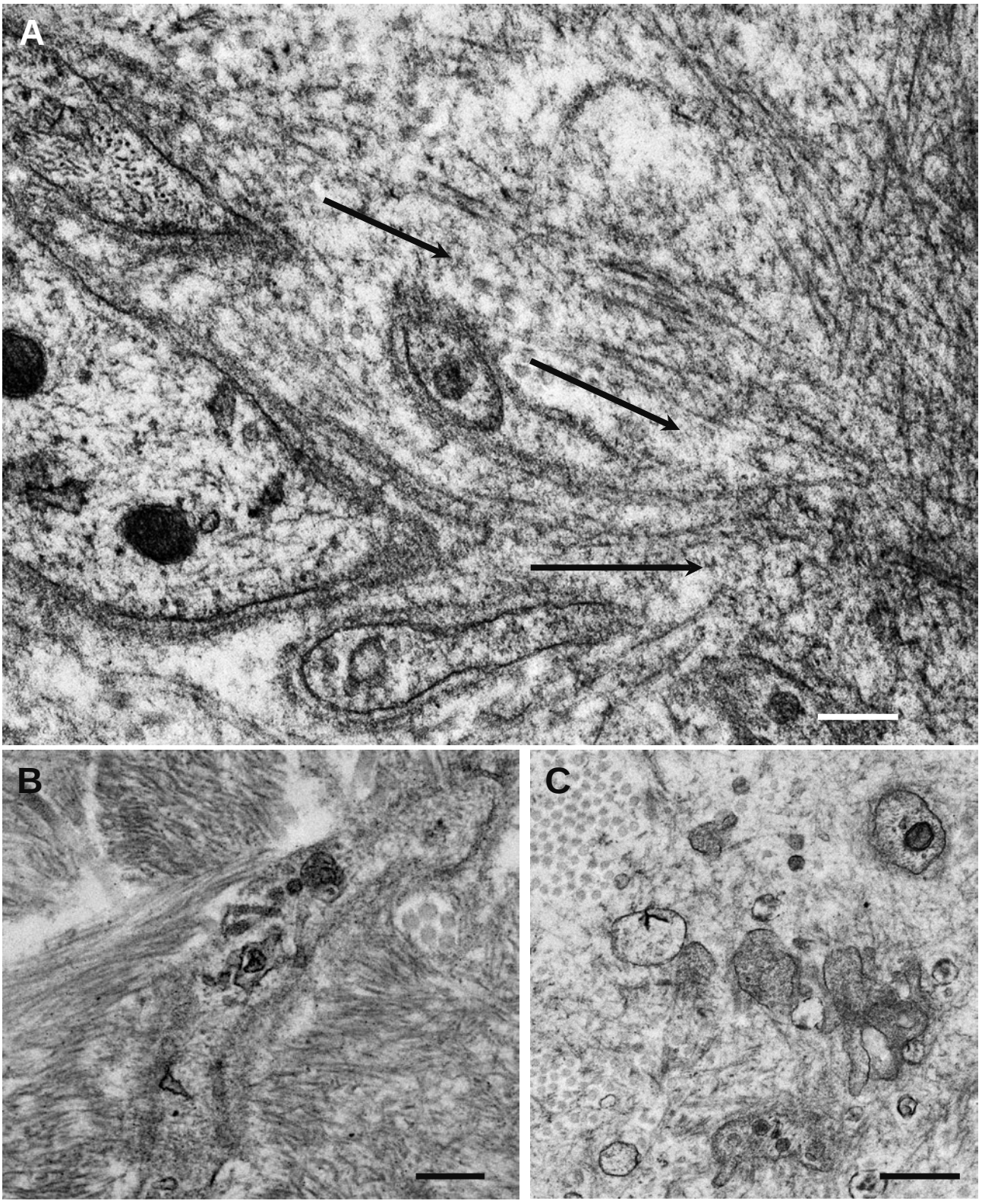

Fig. 4

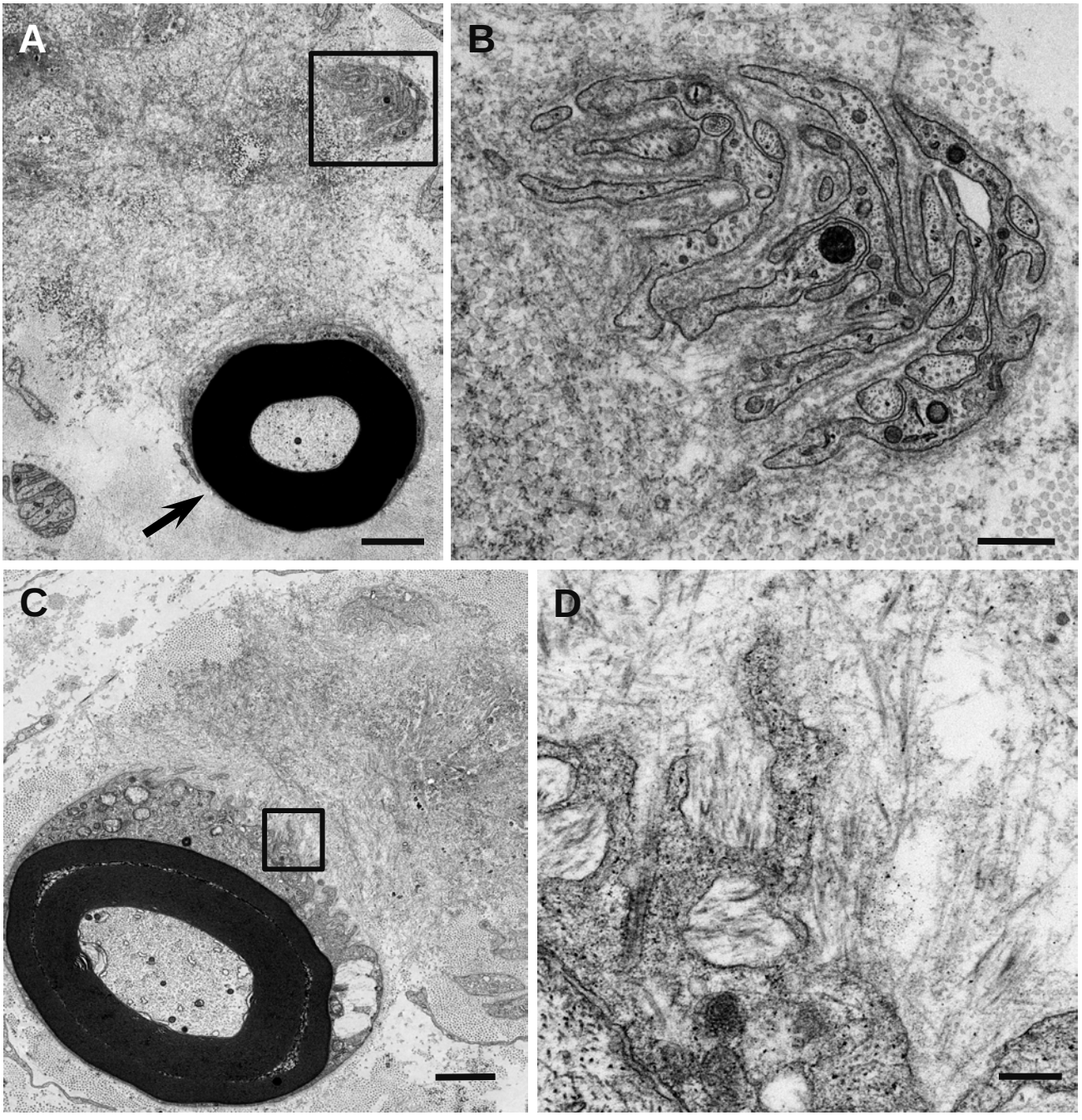

Fig. 5